

Structural and vibrational model for vitreous boron oxide

Rafael A. Barrio

Instituto de Física, Universidad Nacional Autónoma de México, Apartado Postal 20-364, 01000 México, Distrito Federal, Mexico

F. L. Castillo-Alvarado

Escuela Superior de Física y Matemáticas, Instituto Politécnico Nacional, Edif. 9 Unidad Profesional Adolfo López Mateos, 07738 México, Distrito Federal, Mexico

Frank L. Galeener

Department of Physics, Colorado State University, Fort Collins, Colorado 80523

(Received 28 February 1991)

The glass structure of B_2O_3 is thought to contain a large number of threefold six-member regular planar rings. The Raman spectrum shows a highly polarized and very sharp peak at 808 cm^{-1} . A Bethe lattice of boroxol rings is used here to investigate the vibrational density of states and the polarized Raman response. The results reproduce the experimental spectra extremely well and also explain the isotopic shifts of the modes when one substitutes ^{18}O and ^{10}B . Through the calculation of local densities of states in boron or oxygen sites, one could obtain the participation ratio of all the modes, allowing a quantitative examination of the nature of any region in the spectrum, and a comparison with inelastic-neutron-scattering data.

I. INTRODUCTION

Borate glasses are currently of great interest due to their potential use in microelectronic devices. Particularly important is the fact that they become fast ionic conductors when properly doped with alkali metals.¹ There is a well-founded suspicion that this behavior is strongly related to a structural change in the glass,² since the number of oxygen atoms belonging to boroxol rings, as detected by NMR,³ diminishes drastically with doping.

The structure of pure vitreous B_2O_3 is worth studying with care since there is not yet a conclusive model. Some authors⁴ believe that nearly all the boron atoms are in regular B_3O_3 planar rings, and that half of the oxygen atoms serve as bridges between rings. If this is so, this glass represents a beautiful realization of a material with short-range order due to the chemical bonding, and also with intermediate-range order (the boroxol rings), but without long-range order, since it is amorphous. Thus, the main cause of disorder is not wrong bonding, or distortion of the bonds, but the nearly random angle between the plane of a ring and the plane of the B—O—B bridges. Molecular orbital calculations⁵ in a cluster of two isolated boroxol rings show that an angle of 32° between the plane of a ring and the plane of a bridge is favored, although this seems not to be the case in the glass network. There is little dispersion of the B—O—B angles, being 120° in the rings and $\sim 130^\circ$ in the bridges.

In the doped material this regular structure is modified, the boroxol rings disappear linearly with the alkali-metal concentration, and local configurations emerge. The main feature at low concentrations is the creation of tetrahedral boron sites. These sites have been detected by NMR,³ infrared, and Raman⁶ studies, by

which one concludes that there is one tetravalent boron for each alkali-metal atom introduced in the network for concentrations smaller than 0.4. These experiments would be of great help to investigate the structural changes induced by the impurities in the glass, if there were a solid theoretical framework to interpret them. Particularly, Raman-scattering experiments should give valuable structural information once a reasonable model for the vibrations and the Raman response is at hand. The purpose of this paper is to provide a reasonably easy theoretical model to interpret such experiments.

In Sec. II a theory to study the vibrations of a Bethe lattice of boroxol rings is developed, using an extension of the Born Hamiltonian, with central and noncentral forces, and a Green's-function formalism. The vibrational density of states is calculated as the trace of the imaginary part of the Green's function. The Raman response is calculated following a model devised for SiO_2 ,⁷ and an approximate expression to investigate the infrared activity is used. In Sec. III, the results from the theory are discussed and compared with previous theoretical calculations and with the experiments. Finally, in Sec. IV, a summary of the results is presented, and possible extensions of the theory to the doped case are outlined.

II. THEORETICAL MODEL

As a first approximation to model the structure of the glass, one could use the idea of a continuous random network,⁸ which preserves the local coordination of all sites throughout the lattice and has been extremely successful in other materials, as vitreous silica. The main problem when one is interested in a microscopic description of the whole glass is that one cannot state the coordinates of all the atoms, since they are at disordered positions. There-

fore, one has to use a mean-field theory at some stage, if one needs an infinite disordered system, with short-range order only. It is here that the Bethe lattice has proven useful: It has been used to describe the vibrations of a continuous random network of one-component amorphous semiconductors⁹ and of more complicated networks, such as vitreous SiO₂.¹⁰

The case of B₂O₃ is more complicated because of the presence of intermediate-range order in the form of boroxol rings. Since most experimenters believe that the concentration of rings is very high, it is imperative to include them in the network model. Because there are no rings in a Bethe lattice, one can assume that all boron sites "contain" boroxol rings in such a way that one treats a boroxol ring as a single site. If this is the case, one can construct a three coordinated Bethe lattice in which each vertex is a ring. This has been done using a central-forces model¹¹ and including noncentral forces,¹² with limited success.

In this paper we improve the Hamiltonian in order to account for the lack of cylindrical symmetry of the bonds in the rings. It is worthwhile repeating the construction of the Bethe lattice in detail here, since it has never been published before. For a Hamiltonian quadratic in the displacements, the associated Green's function obeys the equations

$$M_{\mu}(l)\omega^2 G_{\mu\mu'}(l,l') = \delta_{\mu\mu'}\delta(l,l') + \sum_{\mu''} \sum_{l''} D_{\mu\mu''}(l,l'') G_{\mu''\mu'}(l'',l'), \quad (1)$$

where M is the mass at site l in the direction of one of the three Cartesian coordinates μ . The matrix of force constants D is formed with the second derivatives of the potential with respect to the Cartesian components of the displacements. In order to solve Eq. (1) for each frequency ω , one must define the structure. Our model will consist in a Bethe lattice of boroxol rings. Figure 1 shows the local arrangement of two boroxol units joined by an oxygen bridge. For a bond along the z axis (direction 1), as the one joining atoms 0 and 1 in the figure, the interac-

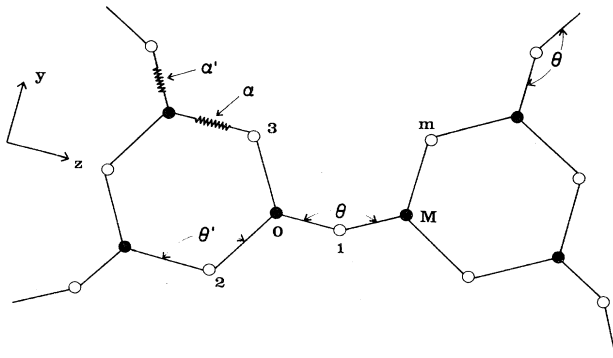


FIG. 1. Geometrical arrangement between two boroxol rings in the B₂O₃ network. When considering atom 0, the z axis is taken in the direction 0-1.

tion matrix is

$$\underline{D}_1 = \begin{pmatrix} \beta_x & 0 & 0 \\ 0 & \beta_y & 0 \\ 0 & 0 & \alpha \end{pmatrix}, \quad (2)$$

where α is the central-force constant, β_x is the orientational restoring force for motions perpendicular to the ring plane (see frame of reference in Fig. 1), and β_y is the orientational restoring force constant for motions in the plane. The Born Hamiltonian contains only one noncentral force β , but this is unrealistic in the case of a ring, since that would mean that the bonds are cylindrically symmetric, which is obviously not the case in the ring. There is a general problem with the Born noncentral force, since it gives a fictitious restoring force for a pure rotational mode due to difference of displacements perpendicular to the bond. These false vibrational modes are encountered only at low frequencies, since β is small.

Let us choose the boron atom 0, attached to the bridge labeled 1 in Fig. 1, and rename it as boron 1, then, omitting the index μ , one writes Eq. (1) using 3×3 matrices for the boron self-correlation \underline{G} as

$$[M\underline{I}\omega^2 + \underline{D}'_1 + \underline{D}_2 + \underline{D}_3] \underline{G}^{11} = \underline{I} + \underline{D}'_1 \underline{g}^{11} + \underline{D}_2 \underline{F}^{21} + \underline{D}_3 \underline{F}^{31}, \quad (3)$$

where M is the boron mass, \underline{D}_2 and \underline{D}_3 are obtained by rotating \underline{D}_1 around the x axis by $3\pi/2$; that is, $\underline{D}_2 = \underline{R}^T \underline{D}_1 \underline{R}$, and the primed matrix means that the force constants of the bond bridging between rings are different from the ones inside the ring. The Green's function \underline{g} is taken between the boron site and the bridging oxygen, and the Green's function \underline{F} is between the boron and the neighbor oxygen in the ring. There are similar equations for \underline{G}^{22} and \underline{G}^{33} . First one can eliminate the coordinates of the oxygen in the ring by defining a 9×9 matrix \underline{W} composed of 3×3 blocks \underline{w} , which are

$$\begin{aligned} \underline{w}_{11} &= M\underline{I}\omega^2 + \underline{D}'_1 + \sum_{j \neq 1} (\underline{D}_j - \underline{D}_j \underline{A}_j^{-1} \underline{D}_j), \\ \underline{w}_{22} &= \underline{R}^T \underline{w}_{11} \underline{R}, \\ \underline{w}_{33} &= \underline{R} \underline{w}_{11} \underline{R}^T, \\ \underline{w}_{12} &= -\underline{D}_2 \underline{A}_2^{-1} \underline{D}_1, \\ \underline{w}_{13} &= -\underline{D}_3 \underline{A}_3^{-1} \underline{D}_1, \\ \underline{w}_{21} &= \underline{w}_{12}^T, \\ \underline{w}_{31} &= \underline{w}_{13}^T, \\ \underline{w}_{23} &= \underline{R}^T \underline{w}_{12} \underline{R}, \\ \underline{w}_{32} &= \underline{R} \underline{w}_{13} \underline{R}^T, \end{aligned} \quad (4)$$

where $\underline{A}_1 = m\underline{I}\omega^2 + \underline{D}_2 + \underline{D}_3$, with m the oxygen mass and $\underline{A}_2, \underline{A}_3$ being $3\pi/2$ rotations of \underline{A}_1 through \underline{R} . Dyson's equation can be written

$$\sum_{k=1}^3 \underline{w}_{jk} \underline{G}^{ki} = \delta_{ij} + \underline{D}'_j \underline{g}^{ji}. \quad (5)$$

When the primed interactions are zero, one gets the

solution for the ring alone $\underline{G}_0 = \underline{W}^{-1}$.

One can further simplify the equations by solving for the self-correlation at the boron site 1,

$$\underline{E}_1 \underline{G}_{nn}^{11} = \underline{I} + \sum_{j=1}^3 \underline{S}_{1j} \underline{D}'_j \underline{g}_{nm}^{j1}, \quad (6)$$

where the subindex n has been introduced to state that all the correlations are taken inside the ring n . The bridging oxygen can be taken to belong to this ring or to the neighbor one, but in this latter case another local frame of reference should be used. The matrices in (6) are defined as

$$\underline{E}_1 = \sum_{j=1}^3 \underline{S}_{1j} \omega_{j1}, \quad (7)$$

$$\underline{S}_{12} = \omega_{13} \underline{r}_3^{-1} \omega_{32} \omega_{22}^{-1} - \omega_{12} \underline{r}_2^{-1}, \quad (8a)$$

$$\underline{S}_{13} = \omega_{12} \underline{r}_2^{-1} \omega_{23} \omega_{33}^{-1} - \omega_{13} \underline{r}_3^{-1}, \quad (8b)$$

$$\underline{S}_{11} = \underline{I}, \quad (8c)$$

and

$$\underline{r}_2 = \omega_{22} - \omega_{23} \omega_{33}^{-1} \omega_{32}, \quad (9a)$$

$$\underline{r}_3 = \omega_{33} - \omega_{32} \omega_{22}^{-1} \omega_{23}. \quad (9b)$$

In order to solve Eq. (6), one needs the equations for the bridging oxygen-boron correlations \underline{g} . Care must be taken to explicitly write the orientation of the bond bridging to the neighbor ring. The \underline{g} for this bond is obtained from the one considered before by an angle θ rotation around an axis perpendicular to the bond direction (which gives the B—O—B angle), followed by an angle ϕ rotation parallel to the bond, which gives the relative orientation of the joint rings. Now the renormalized self-energies depend on the rotations

$$\begin{aligned} \underline{A}'_j(\theta, \phi) &= m \underline{I} \omega^2 + \underline{D}'_j + \phi_j^T \theta_j^T \underline{D}'_j \theta_j \phi_j \\ &= \phi_j^T \theta_j^T \underline{a}_j \theta_j \phi_j, \end{aligned} \quad (10)$$

where $\underline{a}_j = \underline{A}'_j(-\theta, \phi)$.

Thus, the equation of motion for the correlation between any B—O pair is

$$\underline{A}'_j(\theta, \phi) \underline{g}_{nm}^{ji} = \underline{D}'_j \underline{G}_{nm}^{ji} + \phi_j^T \underline{D}'_j \underline{G}_{n+1,m}^{ji}. \quad (11)$$

This equation is written in the frame of reference of ring n , with the z axis oriented along bond j , joining to ring $n+1$.

In the Bethe lattice one must define two transfer matrices, one relating two rings through a bond j ,

$$\underline{T}_j \underline{G}_{nm}^{ji} = \underline{G}_{n+1,m}^{ji}, \quad (12)$$

and another one transferring information to different boron sites within a ring

$$\underline{t}_{jk} \underline{G}_{nm}^{ki} = \underline{G}_{nm}^{ji}, \quad (13)$$

where it is obvious that $\underline{t}_{ii} = \underline{I}$. With these definitions one can immediately solve for a given boron self-correlation (call it site 1 in ring 0)

$$\underline{G}_{00}^{11} = \left[\underline{E}_1 - \sum_{j=1}^3 \underline{S}_{1j} \underline{N}_j \underline{t}_{j1} \right]^{-1}, \quad (14)$$

where $\underline{N}_j = \underline{D}'_j [\underline{A}'_j(\theta, \phi)]^{-1} \underline{D}'_j + \underline{D}'_j \underline{T}_j$. The effective interactions with the exterior of the ring are

$$\underline{D}_j^{\text{eff}} = \underline{D}'_j [\underline{A}'_j(\theta, \phi)]^{-1} \phi_j^T \theta_j^T \underline{D}'_j. \quad (15)$$

There are various ways of analytically solving the equations for the Bethe lattice. A convenient way is to find a complete set of equations for the transfer matrices

$$\underline{D}_1^{\text{eff}} \underline{T}_1 = \underline{D}_1^{\text{eff}} \left[\underline{E}_1 - \underline{D}'_1 \underline{a}_1^{-1} \underline{D}'_1 - \sum_{j \neq 1} \underline{S}_{1j} \underline{N}_j \underline{t}_{j1} \right]^{-1} (\underline{D}_1^{\text{eff}})^T, \quad (16)$$

$$\sum_{i=1}^3 \omega_{ji} \underline{t}_{i1} = \underline{N}_j \underline{t}_{j1}.$$

It is clear that these equations cannot be solved unless all the relative orientations are specified. One can make two reasonable approximations: First one assumes that the angle θ is fixed and the same in all the bridges, and second that the angle ϕ is completely random and statistically independent. As it is, this latter assumption is not essential, and one could treat the problem for another choice of angles, or even for a favored angle. However, the problem becomes scalar when one averages over ϕ , since all the matrices are symmetric. In particular, the ring-to-ring transfer matrix becomes diagonal and its solution is given by

$$\underline{T}_{11} = \underline{T}_{22} = \frac{1}{2} (\underline{H}_{11}^{-1} + \underline{H}_{22}^{-1}), \quad \underline{T}_{33} = \underline{H}_{33}^{-1}, \quad (17)$$

where

$$\begin{aligned} \underline{H} &= \underline{D}'_1^{-1} \theta^T \underline{a}_1 \{ \underline{D}'_1^{-1} [\underline{E}_1 - \underline{S}_{12} \langle \underline{N}_2 \rangle \underline{t}_{21} - \underline{S}_{13} \langle \underline{N}_3 \rangle \underline{t}_{31}] \\ &\quad \times \underline{D}'_1^{-1} \underline{a}_1 - \underline{I} \} \theta \underline{D}'_1^{-1} \end{aligned} \quad (18)$$

and where $\langle \dots \rangle$ means an average over ϕ . The local density at the boron site is given by $\rho_B = -(2M\omega) \text{Im Tr} \underline{G}_{00}^{11} / \pi$, where the Green's function is the ϕ -averaged version of (14). Equations (17) and (18) are solved self-consistently to a desired degree of accuracy. The self-correlations at the oxygen sites can be obtained with the quantities already calculated, for instance, for a bridging oxygen one obtains

$$\underline{G}_{\text{ob}} = (\underline{A}'_1 - \underline{D}'_1 \underline{Z}_1^{-1} \underline{D}'_1 - \theta^T \underline{D}'_1 \underline{Z}_1^{-1} \underline{D}'_1 \theta)^{-1}, \quad (19)$$

where $\underline{Z}_1 = M \underline{I} \omega^2 + \underline{D}'_1 - \sum_{j \neq 1} (\langle \underline{N}_j \rangle - \underline{D}'_j)$ is the effective impedance of the rings. Analogously, one can obtain expressions for the self-correlations of the oxygen in the rings $\underline{G}_{\text{or}}$, although for practical purposes it is better to define a 27×27 matrix for a ring with three oxygen bridges and invert it directly, with Bethe lattices (\underline{Z}) properly attached to the outer bonds. The total density is then written

$$\rho_T = \frac{-2\omega}{3\pi} \text{Im Tr} (6M \underline{G} + 6m \underline{G}_{\text{or}} + 3m \underline{G}_{\text{ob}}). \quad (20)$$

One can also obtain information from the partial densities at a boron site, at an oxygen in the rings, or at a bridging oxygen, with the imaginary parts of \underline{G} , $\underline{G}_{\text{or}}$, or $\underline{G}_{\text{ob}}$, respectively. There are several parameters to adjust,

namely the force constants in the rings α , β_x and β_y , the corresponding force constants for the bridges α' , β'_x , β'_y , and the bridging angle θ . With these many degrees of freedom, one might obtain fairly reasonably looking densities of states for several very different sets of parameters. Therefore, a model for the spectral responses in Raman and infrared experiments is needed.

The model used to obtain the Raman and infrared responses of the Bethe lattice is similar to the one used for vitreous SiO_2 .⁷ There it is shown that the main contribution to the polarized Raman activity is proportional to

$$\omega \text{Im} \left[\sum_{\mu, \nu} \sum_{l, l'} \underline{v}_{\mu}^l G_{\mu\nu}(l, l') \underline{v}_{\nu}^{l'} \right], \quad (21)$$

where \underline{v}_{μ}^l is the μ component of the sum of all the vectors along the bonds arriving to a site l . In principle, the summation over sites should include all the correlations in the Bethe lattice, and this can be carried out; however, one obtains unphysical results. Previous work on SiO_2 has shown that a reasonable picture of the Raman spectrum can be obtained by summing up only the nine sites belonging to a ring and its three bridging oxygens.

In a similar way, it has been shown¹³ that the infrared reflectivity at normal incidence can be calculated from

$$\omega \text{Im} \text{Tr} \left[\sum_{l, l'} e(l) \underline{G}(l, l') e(l') \right], \quad (22)$$

where $e(l)$ is the dynamical charge associated with site l . Since we are interested in looking only at the possibility of infrared activity of a given mode and not at the relative intensities of the peaks, we will not attempt to derive expressions for the dynamical charges, which could be cumbersome and probably inaccurate.¹⁴ Therefore, we use the values ± 1 for the ions, and calculate Eq. (22) in the same cluster as for the Raman.

III. RESULTS

Due to the freedom one has to choose the set of parameters in the theory, the first calculations were made using parameters of previous models in the literature that can be thought of as limiting cases of our theory. Galeener and Thorpe¹⁵ have exhaustively studied the bands obtained from an arbitrary network with a model with central forces only. In particular, they have solved the case of a network containing boroxol rings for an arbitrary value of the bridging angle θ . In Fig. 2(a) there is a sketch of the allowed bands for $\theta=130^\circ$ and $\alpha=470 \text{ N/m}$ (in central forces only, $\beta=0$). There are five bands of s -like states, each with weight $N/3$, six non-dispersive p -like states, which appear as δ functions with weight $N/6$, and one δ function in the middle of the high-frequency band with weight $N/3$. The results of the calculation using the same parameters in our theory are shown in Fig. 2(b), where one can see that the predictions of Fig. 2(a) are found exactly. The bands at very low frequency are the modes driven to $\omega=0$ when all the non-central forces are very small (in the calculation shown in the figure, all the β 's are 0.03, to avoid infinities).

In Fig. 2(c) the calculation of the Raman response is shown, and one notices three bands, one from 450 to 610

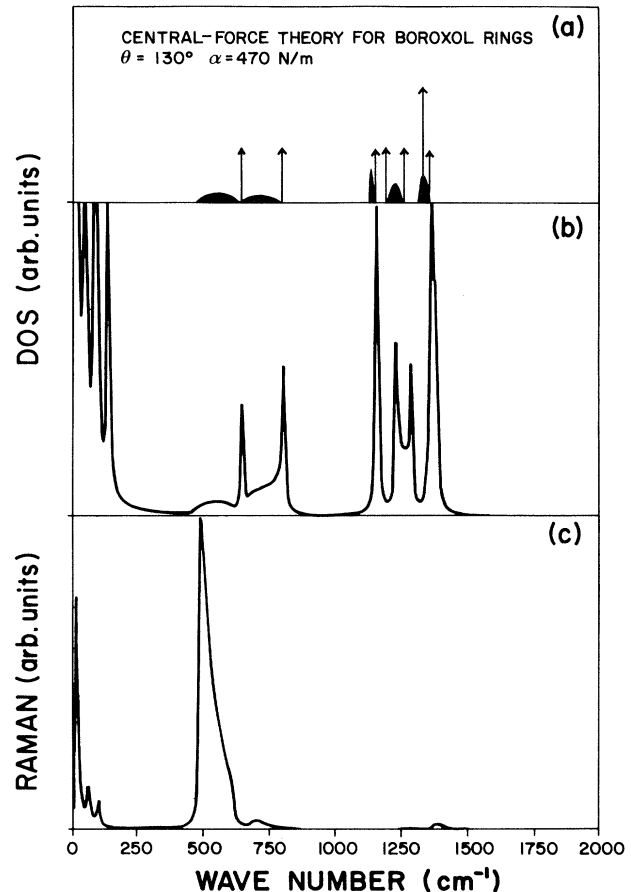


FIG. 2. (a) Schematic representation of the vibrational density of states of a network of boroxol rings, obtained with a central-force model, from Ref. 15. (b) Vibrational density of states calculated using the same parameters as in (a), an imaginary part of 5 cm^{-1} was added to the frequency. (c) The Raman response corresponding to the spectrum in (b).

cm^{-1} , another from 620 to 800 cm^{-1} , and a small one at around 1350 cm^{-1} . The greatest response arises from the lowest band edge, which corresponds to a mode in which all the oxygen atoms breathe in phase. This Raman spectrum does not compare well with the real experiment, in which the main response is found at 808 cm^{-1} . This is not surprising since the central-force model is not able to account for all the modes. The theoretical response is easy to interpret from simple ideas: the bands which exhibit calculated Raman activity are modes in which there is some mixing of the molecular modes of the ring with symmetry A'_1 , and the δ functions are modes which originate from the molecular modes of symmetry E' and A'_2 .

To explore our theory further, we show in Fig. 3 the results of the calculation for the ring along; that is, three boron atoms, three oxygen atoms in the ring, and three exterior oxygen atoms attached to the borons. The irreducible representations of the D_{3h} group give $2A'_1 + 3E' + A'_2$ as true vibrations. The A'_1 modes are Raman active and the three E' modes are infrared active, fulfilling the exclusivity rule for structures with a center

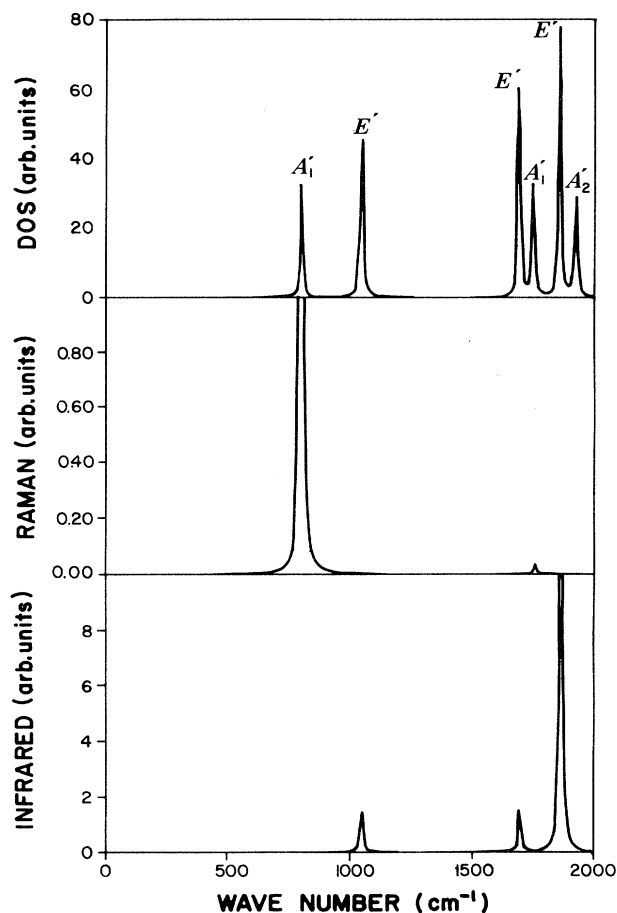


FIG. 3. Molecular modes calculated for an isolated boroxol ring with three outer oxygen atoms. The Raman and infrared activity of the modes, calculated with Eqs. (21) and (22), are also shown.

of symmetry. The A'_2 mode is silent. The value of $\alpha=940$ N/m was chosen in order to compare to the calculation by Kanehisa *et al.*¹¹ who adjusted this value to have the A'_1 mode at 800 cm^{-1} . Unfortunately, when the network is attached to this ring, the effect is to broaden the A'_1 mode to a band, and the sharp peak that appears at 900 cm^{-1} is due to a p -like state, which is not Raman active and does not broaden because it is a nondispersive state in the central-forces model. This means that the apparent fit for $\alpha=940$ N/m is fortuitous, and the true α must have a different value.

The shortcomings of a central-force-only model were pointed out by Galeener and Thorpe¹⁵ some time ago. There is a calculation made with a "ball and stick" handmade model,¹⁶ built to interpret neutron-scattering experiments, in which one value of α and only one value of β are considered for all bonds. That model contained 75% of boron atoms in boroxol rings. In Fig. 4 we reproduce the histogram made in Ref 16 for the total density of states (DOS), together with the result from our model for the appropriate values of $\alpha=420$ N/m, $\beta=0.2\alpha$, and $\theta=120^\circ$. It is seen that the two results compare well: all

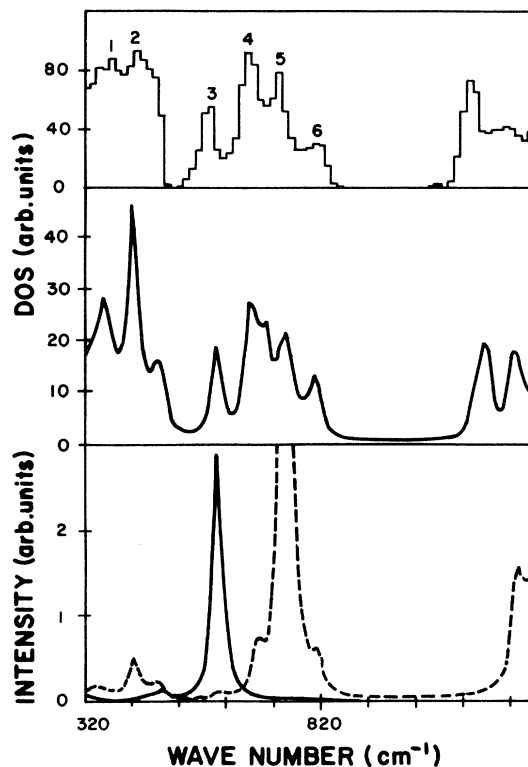


FIG. 4. Comparison between the vibrational density of states obtained with a central-force theory for a ball and stick model (histogram taken from Ref. 16), and the one obtained with the present model for the same set of parameters. The lower section shows the result for the Raman (solid line) and infrared (dashed line) responses for the same model.

the bands with their relative weights are reproduced by the Bethe lattice model, even the relative weight of peaks 4 and 6, which was noted as a virtue of the calculation. Unfortunately, this choice of parameters is not appropriate to explain the Raman response. In order to illustrate this, we show in the lower section of Fig. 4 the result for the Raman and infrared responses from our calculation. Although the infrared spectrum shows the two main peaks at 720 and 1260 cm^{-1} seen in the experiment, the main Raman line at 808 cm^{-1} is found at around 600 cm^{-1} , corresponding to peak 3.

The above comparisons have been useful in order to test our theory. The molecular ring modes are at the predicted frequencies and give the correct Raman and infrared activity, and the Bethe lattice suffices to reproduce the spectra of other models, even when the proportion of boron atoms in the rings is not 100%. The puzzling thing is that not one of these choices give the correct Raman spectrum.

The experimental Raman spectrum of vitreous B_2O_3 (Ref. 17) is shown in Fig. 5, in which the reduced HH and HV polarized spectra are taken from Ref. 12. It is seen that the main feature is a highly polarized peak at 808 cm^{-1} , which is extremely narrow for a glass, and other minor peaks at 470 , 605 , 670 , 732 , 1260 , 1329 , and 1460

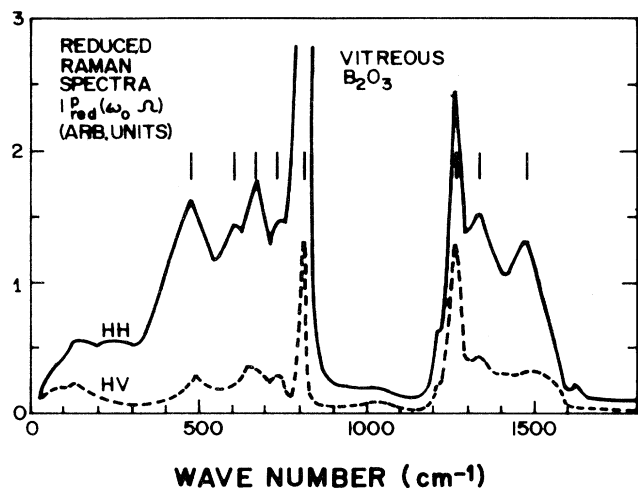


FIG. 5. Experimental polarized Raman spectrum of B_2O_3 , from Ref. 15.

cm^{-1} . The frequencies of all Raman peaks are marked with vertical lines in Figs. 5–7 as a guide to the eye.

In order to get a narrow line at 808 cm^{-1} despite having an infinite network of rings, one has to decouple the A_1' mode of the rings from the rest of the lattice. It has been shown¹⁰ that a certain ratio between the central-

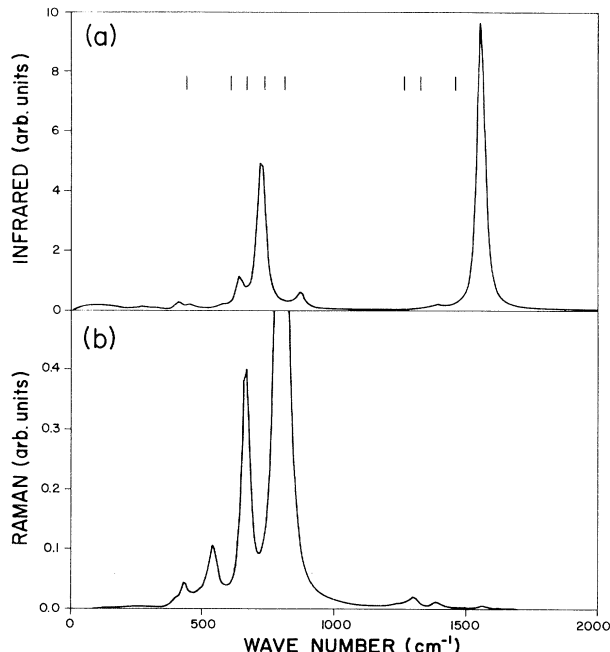


FIG. 7. Theoretical infrared activity (a) and polarized Raman spectrum $\{I_{HH} - \frac{4}{3}I_{HV}\}$ (b) for the density shown in Fig. 6(a).

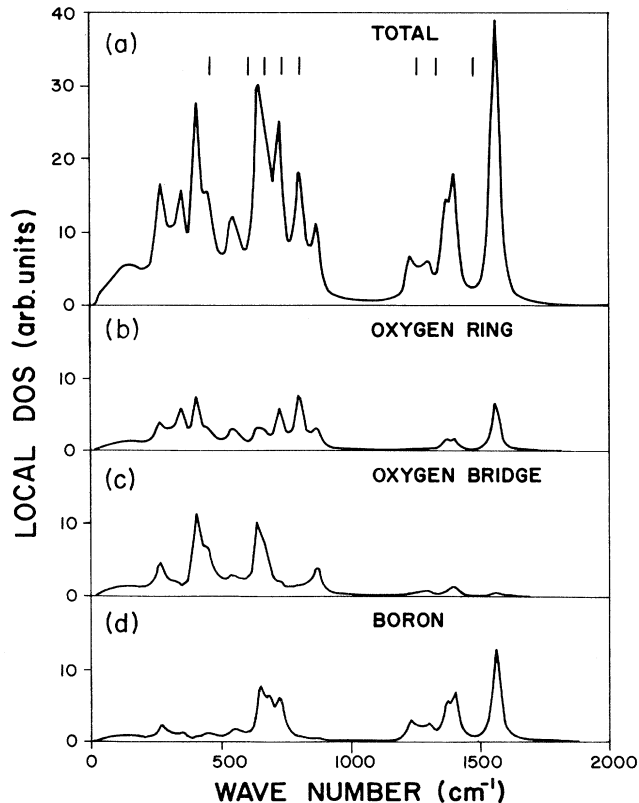


FIG. 6. Theoretical densities of states for B_2O_3 . An imaginary part of 15 cm^{-1} was added to the frequency.

force and the noncentral-force constants gives perfect decoupling of regular planar rings in vitreous SiO_2 . It is easy to show that, for a threefold regular ring with internal angle $\theta' = 120^\circ$, this ratio is $\alpha/\beta = 3$. One has a relative freedom to deviate from the exact value of this ratio, since the calculations show that substantial changes in α/β do not produce a broadening of the peak larger than 15 cm^{-1} [as it was shown for threefold rings in vitreous SiO_2 (Ref. 10)]. With this in mind, the parameters used to fit the vibrational spectrum of B_2O_3 are shown in Table I. The angles are given by experiment,¹² and the force constants varied by trial and error to achieve a best fit. As indicated earlier, primes denote quantities in the bridges between rings.

The fact that we find $\beta_y > \beta_x$ is consistent with our intuition that angular restoring forces in the plane of a B—O—B must be larger than those out of the plane. The fact that primed quantities are generally smaller than unprimed ones reflects the expected greater stiffness of the ring, and the compression of θ' relative to θ .

The partial densities of states at the three different sites in the network, and the total density, from Eq. (20), are shown in Fig. 6. It is seen that the spectrum consists of two bands, separated by a gap from 900 to 1200 cm^{-1} . The upper band is mainly due to boron motion, although a contribution of the oxygen motion in the rings is noticeable, particularly the high-frequency band arising from the broadening of the A_2' ring mode. The motion of the bridging oxygen is confined to the low-frequency band, and a narrow peak, due to oxygen motion, appears at 808 cm^{-1} .

TABLE I. Parameters used.

α	Force constants (N/m)					Angles (deg)	
	β_x	β_y	α'	β'_x	β'_y	θ	θ'
590	78.5	210	320	78.5	100	130	120

In Fig. 7(a) the calculated infrared response is shown, one notices the two main infrared peaks at 714 and 1564 cm^{-1} . There is a small infrared activity from the band around 900 cm^{-1} . These modes are not detected in the experiments, although a hint of the existence of these modes is suggested in the unpolarized Raman spectrum; therefore, one should not regard this as a disagreement between theory and experiment. Figure 7(b) shows the calculated Raman response, the peak at 808 cm^{-1} is the largest feature, as in the experiment. The half-width is around 15 cm^{-1} , and its height is about 50 times larger than the other peaks, as in the experiment. This peak is still reasonably narrow despite of the deviation from perfect decoupling: $\alpha/\beta_y = 2.8$ and $\alpha'/\beta'_y = 3.2$. The other peaks correspond roughly to the observed peaks in Fig. 5, except for the feature at around 720 cm^{-1} . We have examined the frequency shifts of the modes in Fig. 6(a) when the calculation is made with $m = 18$ instead of $m = 16$, and with $M = 10$ instead of $M = 10.8$. In Table II the results of these calculations are compared with the experimental isotopic shifts.

It is seen that, although the frequencies of the modes are in error by as much as 7%, the quite varied calculated isotopic shifts are in impressive agreement with the experiment. The experimental data and the uncertainties were taken from Ref. 15, and the blanks mean that there are no data available. This isotope shift analysis strongly supports our choice of force constants and our identification of atomic motions with experimental peaks.

IV. CONCLUSIONS

The model we have presented for the structural and vibrational properties of pure glass B_2O_3 has the following characteristics.

(1) It includes short-range and intermediate-range order by simulating the amorphous network with a Bethe lattice of regular boroxol rings, which can be solved ex-

actly. It was shown that the fact that, in the real glass, not all the boron atoms form rings is not crucial as far as the vibrational density of states is concerned.

(2) The model is an extension of former simpler models, and one reproduces these models as limiting cases. We believe that the Hamiltonian used is the simplest one that enables one to fit all the experimental features in the vibrational spectra.

(3) The model reproduces reasonably well the frequencies and the participation ratio of the modes, except that the calculated gap is too wide. We believe these discrepancies are both faults of the Born Hamiltonian. The reason for not using a more realistic Hamiltonian, viz., a complete valence force model, is that we are looking for a simple model that captures the behavior of pure B_2O_3 and facilitates future calculations that will include alloying with dopants. We plan to study the vibrational signatures of the changes of structure induced by doping.

(4) Our generalization of the Born Hamiltonian to include different noncentral-force constants for motion in the plane of the ring and out of the plane proves to be useful, since we are able to reproduce the infrared activity of the out-of-plane modes at the correct frequency, with no real complications for the calculation. The final equations turn out to be scalar and the averaging over dihedral angles restores the cylindrical symmetry.

ACKNOWLEDGMENTS

We benefited from useful discussions with M. Kanehisa, M. F. Thorpe, M. Balkanski, and M. Massot. This work was partially supported by the Commission of the European Communities under Contract No. CL1-CT90-0864 (DSCN). F.C.L.A. acknowledges partial support from COFFA, Instituto Politécnico Nacional. F.L.G. is grateful to the Instituto de Física, UNAM, for warm hospitality during a visit to work on this problem, supported by UNAM, DGAPA under Contract No. IN-100-289-UNAM.

TABLE II. Isotopic shifts.

Frequency of the mode for $^{10.8}\text{B}_2^{16}\text{O}_3$ (cm^{-1})		Isotope shifts (cm^{-1})			
		$^{10}\text{B}_2^{16}\text{O}_3$		$^{10.8}\text{B}_2^{18}\text{O}_3$	
Theory	Experiment	Theory	Experiment	Theory	Experiment
430	470	4	0±4	-20	-25
536	500	4	4±4	-24	-28
666	605	2	6±4	-34	-35
714	732	18	18±6	-14	
804	808	0	1±2	-46	-48
1306	1329	42	44±8	-14	-9
1392	1460	39	43±8	-21	-15
1566	1560	40	45±8	-30	

- ¹A. Levasseur *et al.*, *Solid State Ion.* **1**, 177 (1980).
²M. Mossot *et al.* *Mater. Sci. Eng. B* **3**, 57 (1989).
³P. J. Bray, *J. Non-Cryst. Solids*, **95/96**, 45 (1987).
⁴J. Krogh-Moe, *J. Non-Cryst. Solids* **1**, 269 (1969).
⁵N. Uchida, T. Maekawa, and T. Tokokawa, *J. Non-Cryst. Solids*, **74**, 25 (1985).
⁶M. Massot, C. Julien, and M. Balkanski, *Infrared Phys.* **29**, 775 (1989); F. L. Galeener, *Solid State Commun.* **44**, 1037 (1982); F. L. Galeener and A. Geissberger, *J. Phys. (Paris) Colloq.* **43**, C9-343 (1982).
⁷R. A. Barrio, F. L. Galeener, and E. Martínez, *Phys. Rev. B* **31**, 7779 (1985).
⁸J. M. Ziman, *Models of Disorder* (Cambridge University, Cambridge, 1979), p. 64.
⁹R. A. Barrio, R. J. Elliott, and M. F. Thorpe, *J. Phys. C* **16**, 3425 (1983).
¹⁰F. L. Galeener, R. A. Barrio, E. Martínez, and R. J. Elliott, *Phys. Rev. Lett.* **53**, 2429 (1984).
¹¹M. A. Kanehisa and R. J. Elliott, *Mater. Sci. Eng. B* **3**, 163 (1989).
¹²R. A. Barrio and F. L. Galeener, in *Anais do Simposio Latino-Americano de Física dos Sistemas Amorfos*, edited by E. Anda (Centro Latino-Americano de Física, Rio de Janeiro, 1985), Vol. II, p. 381.
¹³F. L. Galeener, A. J. Leadbetter, and M. W. Stringfellow, *Phys. Rev. B* **27**, 1052 (1983).
¹⁴W. A. Harrison, *Electronic Structure and the Properties of Solids* (Freeman, San Francisco, 1980), p. 273.
¹⁵F. L. Galeener and M. F. Thorpe, *Phys. Rev. B* **28**, 5802 (1983).
¹⁶A. C. Hannon, R. N. Sinclair, J. A. Blackman, Adrian C. Wright, and F. L. Galeener, *J. Non-Cryst. Solids* **106**, 116 (1988).
¹⁷F. L. Galeener, G. Lucovsky, and J. C. Mikkelsen, Jr., *Phys. Rev. B* **22**, 3983 (1980).